Title

Comparison of Ganglion Cell Layer and Inner Plexiform Layer Rates of Change in Suspected and Established Glaucoma.

Authors

Mohammadi, Massood
Su, Erica
Chew, Leila
et al.

Publication Date

2023-05-01

DOI

10.1016/j.ajo.2022.12.008

Peer reviewed

HHS Public Access

Author manuscript

Am J Ophthalmol. Author manuscript; available in PMC 2023 May 01.

Published in final edited form as:

Am J Ophthalmol. 2023 May ; 249: 12–20. doi:10.1016/j.ajo.2022.12.008.

Comparison of Ganglion Cell Layer and Inner Plexiform Layer Rates of Change in Suspected and Established Glaucoma

Massood Mohammadi[1], **Erica Su**[2], **Leila Chew**[1], **Vahid Mohammadzadeh**[1], **Joseph Caprioli**[1], **Robert E. Weiss**[2], **Kouros Nouri-Mahdavi**[1]

[1]Glaucoma Division, Stein Eye Institute, David Geffen School of Medicine, University of California Los Angeles, Los Angeles, California

[2]Department of Biostatistics, Fielding School of Public Health, University of California Los Angeles, Los Angeles, California

Abstract

PURPOSE: We compared ganglion cell layer (GCL) and inner plexiform layer (IPL) rates of change (RoC) in patients with suspected (GS) and established glaucoma (EG) to test the hypothesis that IPL thickness changes occur earlier than GCL in eyes with early damage.

DESIGN: Prospective, cohort study.

METHODS: 64 GS eyes (46 patients) and 112 EG eyes (112 patients) with ≥2 years of follow-up and ≥3 macular optical coherence tomography scans were included. GCL and IPL superpixel thickness measurements were exported. A Bayesian hierarchical model with random intercepts/slopes, and random residual variances was fitted to estimate RoC in individual superpixels. Normalized RoC and proportions of superpixels with significantly negative and positive GCL and IPL RoC were compared within the groups.

RESULTS: Average (SD) follow-up time and number of scans were 3.5 (0.7) years, and 4.2 (1.0), respectively, in the GS group and 3.6 (0.4) years and 7.3 (1.1) in the EG group. Mean (SD) normalized RoC was faster for GCL than IPL (−0.69 [0.05] vs. −0.33 [0.04]) in the GS group, whereas it was faster for IPL (−0.47 [0.03] vs. −0.28 [0.02]) in EG eyes. GCL RoC were significantly negative in 24/36 superpixels compared with 8/36 for IPL ($p<0.001$) in GS eyes. In the EG group, 23/36 superpixels had significant negative IPL RoC compared to 13/36 superpixels for GCL ($p=0.006$).

CONCLUSIONS: GCL thickness was more likely to demonstrate change compared to IPL in glaucoma suspects. There is no evidence of preferential IPL thinning in eyes with suspected early glaucoma damage.

Table of content statement

Corresponding author: Kouros Nouri-Mahdavi, MD, MS, 100 Stein Plaza, Los Angeles, CA, 90095, USA, Phone: 310-794-1487, Fax: 310-794-6616, nouri-mahdavi@jsei.ucla.edu.

Two groups of patients, one with suspected the other with established glaucoma, were longitudinally followed with macular OCTs to evaluate if inner plexiform layer is preferentially lost in very early glaucoma. Our results showed that ganglion cell layer displayed faster rates of decline in glaucoma suspect eyes while inner plexiform layer rate of loss was faster in the established glaucoma group. Ganglion cell layer is the preferred biomarker for change detection in suspected/very early glaucoma.

Keywords

Optical Coherence Tomography; OCT; macula; ganglion cell layer; GCL; inner plexiform layer; IPL; longitudinal; Bayesian; hierarchical; superpixels; early detection

Introduction

Axonal injury at the level of the optic nerve head leads to apoptosis and loss of retinal ganglion cells (RGC) in glaucoma.[1] Inner macular measurements have shown promise for both early detection of the disease and monitoring glaucoma progression at different stages of the disease. With improving resolution of optical coherence tomography (OCT) imaging devices, the features and alterations of individual macular layers can be better explored in normal and glaucoma subjects.[2–6]

Experimental studies have indicated that early RGC axonal injury results in dendritic changes including dendrite retraction, reduced arborization, and synaptic loss.[7–11] Retinal ganglion cells demonstrating such changes are considered to be at high risk of apoptosis during the course of glaucoma. These findings have drawn interest in identifying changes in the IPL thickness as a potential biomarker for detection of early glaucomatous damage. A few recent cross-sectional studies with current OCT devices have assessed IPL thickness and its correlation with visual field loss or GCL thickness in glaucoma patients.[12–15] The results of these studies have not been consistent as to the utility of IPL thickness as a biomarker for early glaucoma detection. High-resolution OCT imaging with visible light was recently shown to be able to delineate the IPL sublayers and their pattern of change in a small group of glaucoma eyes; [16] this novel finding points to the potential utility of the IPL thickness measurements for monitoring glaucoma.[17]

The goal of the current study is to assess and compare the rates of change (RoC) of IPL and GCL thickness in two cohorts of patients with suspected or established glaucoma to better delineate the respective changes in these two layers over time at different stages of the disease.

Methods

The current investigation included subjects from 2 cohorts of patients who have been followed the Department of Ophthalmology, University of California Los Angeles (UCLA). This study was carried out in accordance with the tenets of the Declaration of Helsinki and the Health Insurance Portability and Accountability Act (HIPAA) and was approved by the UCLA Human Research Protection Program.

Participants

Glaucoma suspect cohort.—We reviewed records of 755 eyes of 386 patients identified as glaucoma suspects based on ICD-9 diagnostic parent code 365.0 and ICD-10 parent code H40.0 who were seen by a single glaucoma specialist (KNM) from March 2014 to December 2020. These patients were diagnosed as glaucoma suspect based on suspicious optic disc appearance or ocular hypertension and were followed over time at regular intervals. The former group of eyes showed findings such as large vertical cup-to-disc ratio, violation of the ISNT (Inferior-Superior-Nasal-Temporal) rule or cup-to-disc asymmetry as ascertained by the examining clinician. The eligible eyes had normal achromatic visual field exam and normal retinal nerve fiber layer findings on OCT imaging at baseline and did not demonstrate progression during the follow-up period (see progression criteria below).

Other inclusion criteria were as follows: 1) baseline best-corrected visual acuity of 20/30 or better, 2) axial length <26.5 mm or refractive error of −6 or less, and 3) a minimum of 2 years of follow-up and 3 or more macular OCT scans with no coexisting retinal and optic nerve head pathologies. Glaucoma progression was identified under the following circumstances: 1) development of glaucomatous optic nerve changes such as localized thinning or notching, development of new or extension of previous peripapillary retinal nerve fiber layer (RNFL) defect, disc hemorrhage, (increased) asymmetry of vertical cup-to-disc ratio; 2) global RNFL rates of decline faster than 1 μm/year; or 3) confirmed evidence of glaucomatous visual field conversion manifested during the follow-up defined as Glaucoma Hemifield Test outside normal limit or 4 or more abnormal points with p values <0.05 on pattern deviation plot on 24–2 Swedish Interactive Thresholding Algorithm standard visual field test.[18]

Patients underwent ophthalmic examination including determination of best-corrected visual acuity, intraocular pressure measurement with Goldmann applanation tonometry, central corneal thickness measurement, visual field (VF) evaluation and OCT examination at baseline and were followed every year with OCT scans and visual field tests.

Established glaucoma group.—We recruited patients from the Advanced Glaucoma Progression Study (AGPS), a longitudinal, prospective study at the Stein Eye Institute, University of California Los Angeles (UCLA). The cohort has been described previously.[19] To be included in the current study, the enrolled eyes had to have at least two years of follow-up with ≥3 macular OCTs. Eyes enrolled in the AGPS were also required to meet the following criteria: 1) visual field mean deviation (MD) of −6.0 decibels (dB) or worse or central VF involvement as evidenced by the presence of ≥2 test locations with p <0.05 on the pattern deviation plot within the central 10 degrees on the 24–2 VFs confirmed at least once. Patients underwent clinical exam, OCT imaging and VF testing every 6 months.

OCT imaging

The Posterior Pole Algorithm of the Spectralis SD-OCT was used for macular scanning. This algorithm acquires 30°×25° volume scans of the macula centered on the fovea. It consists of 61 horizontal B-scans each comprised of 768 A-scans. Nine to 11 B-scans are averaged to decrease speckle noise and improve image quality. The central 24°×24°

of the volume scan was segmented by the Glaucoma Module Premium Edition software and its data presented in an 8×8 array of 3°×3° superpixels. For this study, the macular layers of interest were IPL and GCL. We chose the central 6×6 superpixels for analysis due to the lower average thickness and increased variability and noise of the more peripheral superpixels (Supplementary Figure 1).

In both GS and EG groups, low quality macular SD-OCT images such as those with quality factor <15 or major artifacts were excluded. The OCT image segmentation in the EG group was previously corrected by reviewers. The GS cohort database is a more recent cohort and met all the quality criteria. A recent audit of data in our lab demonstrated that correction of segmentation does not appreciably affect estimated RoC. We also excluded the outer rows and columns of the macular superpixels in this study, which are more prone to segmentation errors. Therefore, we decided not to manually correct image segmentation in the GS group. Data were exported as XML files, and the right eye format was used for all eyes.

Retinal nerve fiber layer (RNFL) was measured with a single circular OCT scan, 12° in diameter, centered on the optic disc (768 individual A-scans). Segmentation was visually checked and adjusted manually as required and only scans with quality scores ≥15 without other artifacts were included in the analysis.

After considering exclusion criteria based on clinical characteristics and also OCT image quality checks,112 eyes of 112 patients were included in the current study as the EG group. Furthermore, 64 eyes of 46 patients satisfying the inclusion and exclusion criteria were included for analysis as the GS cohort.

Statistical analyses

Our methods have been reported on elsewhere for the AGPS data.[20] Exploratory graphical analysis followed methods described in Weiss.[21] Visits within 2 months of a previous visit were excluded. For both IPL and GCL and for both GS and EG cohorts, we omitted individual eye-superpixel observations as outliers if there was a large change from the previous visit and to the following visit, omitting about 0.5% of all measurements. A complete description of the algorithm is given in the Appendix. For each cohort, superpixel, and outcome, we fit a Bayesian hierarchical random effects model with population intercept and rate of change, patient-specific random intercepts and rates of change, and a patient-specific residual variance. For the GS cohort, we also included eye random intercepts and RoC. Intercepts and RoC are correlated a priori, but patient and eye random effects are a priori independent. In the EG group, we also fit a model with a mean deviation (MD) group main effect and MD group by time interaction, where MD groups were MD ≤ −6 dB versus MD >−6 dB. We fit each model with JAGS in R using Markov Chain Monte Carlo with 3 chains of length 250,000 with a burn-in of 50,000 and a thinning of 40, producing posterior samples of size 15,000 with satisfactory convergence and mixing.[22,23,24] We estimated the global rates of change for RNFL measurements for both cohorts with these same models. The data for global RNFL rate estimation were available for 110 EG eyes and 57 GS eyes.

We calculated posterior means, SDs, and 95% central credible intervals (CrI) for parameters of interest. For each superpixel, we calculated the one-sided Bayesian p value for average

population RoC as the posterior probability that the coefficient was negative; the superpixel average population RoC was considered significantly negative (positive) if the posterior probability that the slope was negative (positive) and greater than 0.975 (less than 0.025). Since 18 patients from the GS cohort contributed both eyes to the cohort, the overall eye RoC (hereafter just *eye RoC*) is the sum of the population RoC plus the patient specific random RoC plus the eye specific random RoC. The eye RoC for the EG cohort are the sum of the population RoC plus their random RoC. We identified an eye-superpixel RoC as significantly negative (positive) if the posterior probability that the RoC is negative (positive) was greater than 0.9 (less than 0.10). We used a more stringent criterion for the average population RoC in superpixels because the data contains a substantial amount of information about population RoC and we used a less stringent criterion for individual eye-superpixel RoC because there is much less information about individual eye-superpixel RoC.

We defined standardized rates of change for each superpixel/eye as the RoC divided by the standard deviation of the random RoC across eyes and summarized standardized RoC as for the RoC. For the EG cohort, the SD of the random RoC is the posterior mean of the square of the RoC random effect variance, while for the GS cohort, the SD of the random RoC is the posterior mean of the square root of the sum of the subject RoC random effect variance plus the eye RoC random effect variance.

For both cohorts, by superpixel and overall, we compared GCL and IPL on eye RoC and standardized RoC by calculating, for each posterior sample, the fraction of GCL (standardized) eye RoC that were more negative than IPL (standardized) eye RoC; we then summarized the posterior distribution of this fraction as a posterior mean, SD, and 95% credible interval (CrI). For both cohorts and for each superpixel, we calculated the proportion of significant GCL and IPL negative RoC and compared these proportions with McNemar's test and report two-sided classical p values. For the GS cohort, we selected a random eye for subjects with two eyes included before running McNemar's test.

For both cohorts, we tabulated the number of eye-superpixel RoC that were significantly negative in both, in only one or neither IPL or GCL and displayed these numbers in Venn diagrams. The number of eye-superpixels for the GS cohort is 64 * 36 = 2304 while for established glaucoma the number is (112 * 36) − 4 = 4028 as 4 superpixels did not have data to use to calculate both slopes.

Results

Study population

Sixty-four eyes of 46 glaucoma suspect patients and 112 eyes of 112 patients with established glaucoma were included in this study. Table 1 summarizes the demographic and clinical data for the two groups. The average (SD) RoC of global RNFL was − 0.49 (0.29) μm/year in the GS group and −0.61 (0.74) μm/year in the EG cohort. Sixty-four EG eyes were enrolled in the study based on having severe glaucoma (MD ≤−6 dB) and 48 eyes were included based on having central visual field damage as described in Methods. All eyes that satisfied the severity criterion also met central field involvement criteria.

GCL and IPL rates of change

In the GS cohort, the average normalized RoC (SD) for GCL was more than 2 times faster than that of IPL (−0.69 [0.05] vs. −0.33 [0.04], respectively). In the established glaucoma patients, the normalized mean RoC(SD) was faster for IPL than GCL (−0.47 [0.03] vs. −0.28 [0.02], respectively). Figure 1 plots each superpixel's mean population RoC for IPL versus GCL in the GS and EG groups. In the GS group, the GCL population average RoC is more negative than the IPL population average RoC in most superpixels, while in the established glaucoma group, IPL RoC was more negative than GCL RoC.

MD Subgroup analysis-—In the EG group, the GCL or IPL RoC were not different between the 2 subgroups with visual field MD >−6 dB and MD ≤−6 dB in 35 of 36 superpixels. The GCL superpixel with significantly different RoC between the two groups was different from the IPL superpixel with a significant different RoC (Supplementary Figure 2). The subgroup with MD ≤−6 dB, had a significantly lower intercept for GCL in 27/36 superpixels and for IPL in 13 superpixels compared with the subgroup with MD >−6dB (Supplementary Figure 3).

Superpixels with significant negative and positive rates of change

In the GS cohort, 24 out of 36 superpixels had significantly negative average population RoC for GCL; in contrast, 8/36 superpixels had significantly negative IPL average population RoC (see Supplementary Figure 4, McNemar's test for the difference $p < 0.001$). In the EG group, 13 out of 36 superpixels had significantly negative average population GCL RoC vs. 23/36 superpixels for IPL (McNemar's test for the difference $p = 0.006$; Supplementary Figure 4). In the GS cohort, only one superpixel had a significant positive average population RoC for IPL and no superpixel had a positive average population RoC for GCL; in the established glaucoma group, no superpixel showed significant positive average population RoC for IPL or GCL.

Venn diagrams displaying the count of eye-superpixel- with significantly negative RoC for both for the GS and EG groups, for just one, or for neither of IPL nor GCL are shown in Figure 2. A higher percent of eye-superpixels displayed significant GCL thinning only (23%) compared with IPL thinning only (6%) in the GS cohort with a small number of eye-superpixels with significant decline in both GCL and IPL thickness (3%). In the EG group, the percent of eye-superpixels with significantly declining IPL thickness only (13%) was slightly higher than those displaying significant GCL only worsening (10%). The EG group had 8% eye-superpixels significantly declining on both GCL and IPL while GS only had 3%.

Proportion of eyes significantly worsening in each superpixel

The proportion of eyes with a significant negative RoC in each of the 36 central superpixels is plotted for GCL and IPL for both cohorts in Figure 3. In the GS group, in 18 out of 36 superpixels this proportion was significantly higher for GCL while in 2/36 superpixels the IPL proportion was significantly higher. In the EG group, GCL had significantly higher proportions of significantly negative RoC in 4 out of 36 superpixels while 12/36 superpixels had significantly greater proportions for IPL.

The proportion of eyes with GCL declining faster than IPL in each superpixel is shown in Figure 4 with the corresponding 95% CrI. In most superpixels GCL had a higher probability of faster thinning than IPL in the GS group; in 8 out of 36 superpixels, this probability was statistically significant. In the EG group, for most superpixels, IPL was more likely to have faster thinning than GCL and in 9 superpixels this faster rate was statistically significant.

Discussion

We demonstrated that in a group of eyes with suspected glaucoma, GCL thickness declined more rapidly than IPL with no indication for preferential IPL loss. The GS group, a patient sample with suspected or very early glaucomatous optic neuropathy, GCL showed faster rates of thinning compared to IPL, and a larger number of superpixels in the central macula demonstrated higher probability of faster GCL RoC compared to IPL. On the other hand, in eyes with established glaucoma, IPL displayed relatively faster rates of decline than GCL, and a greater number of macular superpixels had faster IPL RoC than GCL.

Injury at the level of optic nerve axons results in signaling cascades that eventually culminate in RGC death.[25] Macular OCT imaging is useful for monitoring glaucoma thanks to its ability to delineate and measure various components of the RGC axonal complex within the central macula with high reproducibility.[3] Recently, in a longitudinal study in mice, Henderson showed that in chronic experimental glaucoma, dendritic changes occur over time proportionately to the level of IOP elevation.[26] Previous experimental studies showed similar findings in the dendritic arbor of RGCs, which had sustained high IOP. The ability to detect these dendritic changes in a timely manner in glaucoma would not only be diagnostically important but it may also be therapeutically appealing; Agostinone et. al.[27] reported that therapeutic strategies such as human recombinant insulin, administered after dendritic arbor retraction and prior to RGC death, can lead to regeneration of dendrites and reconnection with presynaptic cells. Consequently, there is growing interest in identifying IPL changes in glaucoma as a biomarker for early glaucomatous damage or its progression.

Our study comprises two cohorts of patients with different levels of glaucomatous damage. The GS cohort consisted of a group of patients of suspected glaucoma with normal RNFL thickness at baseline and a very slow rate of loss in global RNFL thickness (−0.49 μm/year); such eyes were also required to have a normal visual field at baseline (MD = −0.5 dB) and throughout the follow-up. On the other hand, the glaucoma (EG) group in our study included patients with central or moderate to advanced glaucoma damage (MD = −8.4 dB).

Findings of studies evaluating the diagnostic performance of IPL thickness in glaucoma have been inconsistent. Kim et al. and Chein and colleagues evaluated IPL's diagnostic power compared to other layers of the inner macula and found that it had a lower area under the ROC curve than GCL for discriminating glaucoma from normal subjects.[12,28] In our prior work with a cross-sectional design, we could not find any evidence for preferential thinning of IPL in glaucoma patients compared to GCL.[14] On the other hand, some studies showed that IPL thickness had a stronger association with visual field sensitivities than GCL.[13] With customized macular scans, Aydin et. al. recently showed that a decline in IPL

thickness and IPL density, as opposed to unchanged or increased IPL thickness or density, was significantly associated with corresponding visual field worsening.[15]

The current paradigm for structural evaluation of glaucoma with OCT devices is mainly based on thickness measurement as a biomarker for damage to various structures in the posterior pole of the eye such as the RNFL, optic nerve head, and inner macular layers. However, identifying changes in the RGC dendritic arbor, which is located in the IPL, as shown in early experimental glaucoma, may require devices with higher resolution or using measures other than thickness such as layer or sublayer reflectivity or density. Ghassabi et al.[16] recently used visible light OCT to demonstrate that it is possible to visualize sublayers of the IPL, which correspond to the previously reported histologic studies. However, based on our findings, dendritic alterations in IPL cannot be picked up earlier than GCL thickness changes by current OCT devices in eyes with suspected or very early glaucoma.

In our current study, GCL thickness showed a consistently faster rate of thinning in the GS cohort compared with IPL. Glaucoma suspect eyes have been shown in a number of studies to progress more slowly than eyes with early glaucomatous damage but faster than normal eyes.[29, 30] The age-related decline in various structural measures has been previously described in the literature.[31–33] Chauhan et. al reported that average GCL and IPL rates of decay in healthy individuals were −0.11 μm/year and −0.07 μm/year, respectively.[31] The GCL and IPL RoC in most superpixels in our GS group showed a faster rate of decline (supplementary Figure 4). Furthermore, our GS group's global RNFL RoC was −0.49 μm/year, which is faster than those reported for normal subjects in prior studies.[34–36] Chauhan et al. reported an age-related global RNFL rate of thinning of about −0.20 μm/year. [31] As we capped the rates of global RNFL at −1 μm/year for inclusion in the study, the GS group's RoC for global RNFL was somewhat lower than those reported by Miki et. al. and Bowd and collaborators in their glaucoma suspect groups (−0.8 to −0.6 μm/year).[30,34] Even if the identified changes in our GS cohort were purely a function of aging, faster age-related GCL thinning would mean that GCL is likely be the preferred biomarker for identifying early glaucomatous damage compared to IPL since glaucomatous damage follows a similar pattern compared to age-related RGC and RNFL decay.[31,37]

In the current study, EG patients consisted of treated glaucoma patients who showed progressive global RNFL RoC of −0.61 μm/year. We found that the IPL RoC were relatively faster than GCL and the probability of faster IPL thinning was higher in more macular superpixels although the difference between the two measures was less compelling in the EG cohort than in the GS cohort. Another interpretation of our results is that it is possible that the IPL thinning may accelerate with worsening of glaucoma, which seems to contradict the possibility of early pruning of the RGC dendrites.

We observed only a partial overlap between the superpixels showing significant thinning of the IPL vs. those demonstrating significant GCL thinning. This confirms the utility of combined thickness measures (e.g., GCIPL or GCC) in monitoring of glaucoma patients as the RoC of the combined layers may provide more information than the individual layer RoC across the spectrum of glaucoma. Because our GS cohort had two eyes from some patients included, we utilized a model with additional components to accommodate the

pairing of eyes for the GS patients as compared to the model for established glaucoma patients who only contributed measurements from one eye. We found that the between-eye variance was smaller than the between patient variance, indicating moderately high correlation (>0.5) of GCL and IPL levels and rates of change between paired eyes.

The results of our study should be interpreted considering its limitations. Segmentation of IPL can be challenging for the current OCT devices as the reflectivity gradient between the IPL and GCL tends to be lower compared to its contrast with the inner nuclear layer. It is possible that with the higher resolution of future OCT generations, a more nuanced explanation may be discovered. In both groups, the quality of the images were the main criteria for inclusion with emphasis on excluding any images with macular pathology. Recent unpublished findings from our lab have shown that manual correction of segmentation does not affect the estimated rates of change. The layer segmentation in the EG group, which is an older database, was originally lightly corrected by human reviewers. The GS cohort database is a more recent cohort and met all the quality criteria as detailed in the manuscript; based on our recent findings, we decided to not manually correct image segmentation. Also, the automated segmentation task is much less challenging and prone to errors in eyes with normal or near normal retinal layer thickness measurements such as in the GS group.

In summary, our study provides evidence that GCL thickness is the superior macular structural biomarker, compared to IPL, for detection of earliest signs of glaucoma in the macular region. In the more advanced stages, IPL tended to show relatively faster rates of thinning. Our findings suggest that evidence of early pruning of the dendritic arbor as manifested by thinning of the IPL cannot be corroborated in human glaucoma with the current resolution of OCT imaging.

Supplementary Material

Refer to Web version on PubMed Central for supplementary material.

Acknowledgements and Financial Disclosure

Funding/Support:

This study was supported by a National Institutes of Health R01 grant (EY027929), an unrestricted Departmental Grant from Research to Prevent Blindness, and an unrestricted grant from Heidelberg Engineering (KNM).

Financial Disclosures:

K.N-M. received grants from the National Institutes of Health and an unrestricted grant from Heidelberg Engineering, Inc. J.C. discloses relationships with Aerie Pharmaceuticals, Alcon, Allergan, Glaukos Corporation, New World Medical, Simms/Mann Family Foundation, and Payden Fund. All other authors indicate no financial support or conflicts of interest.

Appendix

Outlier Removal Process

For each layer in each cohort, we applied our semi-automated process independently to identify and remove outliers. Let y_{ijk} denote the thickness of the layer on subject i measured at the jth visit of subject i at time t_{ij} in superpixel k for $k = 1, \ldots, K$. Time since baseline t_{ij} is measured in years, where the first visit for all subjects is at $t_{ij} = 0$ years. For each patient at each superpixel, we calculated consecutive visit absolute differences $|y_{ijk} - y_{i(j-1)k}|$ and consecutive visit absolute centered slopes $|(y_{ijk} - y_{i(j-1)k})/(t_{ij} - t_{i(j-1)}) + \mu|$; slopes were centered around μ, the mean of the pooled set of slopes from all pairs of consecutive visits across all patients and superpixels. The means for centering were −0.14, −0.19, −0.20, and −0.08 μm/y for EG-GCL, EG-IPL, GS-GCL, and GS-IPL, respectively. We flagged absolute centered slopes greater than 15 and 11 μm/y for GCL and IPL, respectively, with consecutive visit absolute differences greater than 5 μm. These values were chosen to remove approximately 0.5% of the observations as outliers. The flagged slope identified 2 consecutive points as candidates for removal. We calculated the sum of the absolute visit differences $\sum_{j=2}^{n_{ik}} |y_{ij} - y_{i(j-1)}|$ for each patient for each superpixel and further considered the candidate that caused the largest decrease in the sum of the absolute visit differences. If removing the candidate resulted in a replacement absolute slope that was not one-half or less of the original flagged slope, we did not remove the observation; otherwise, we removed the candidate. If an observation was removed, we applied the same algorithm to the reduced dataset to see whether another observation from the same superpixel should be removed as well.

References

1. Weinreb RN, Khaw PT. Primary open-angle glaucoma. Lancet. 2004;363(9422):1711–1720. doi:10.1016/S0140-6736(04)16257-0 [PubMed: 15158634]
2. Zeimer R, Asrani S, Zou S, Quigley H, Jampel H. Quantitative detection of glaucomatous damage at the posterior pole by retinal thickness mapping. A pilot study. Ophthalmology. 1998;105(2):224–231. doi:10.1016/s0161-6420(98)92743-9 [PubMed: 9479279]
3. Tan O, Li G, Lu ATH, Varma R, Huang D, Advanced Imaging for Glaucoma Study Group. Mapping of macular substructures with optical coherence tomography for glaucoma diagnosis. Ophthalmology. 2008;115(6):949–956. doi:10.1016/j.ophtha.2007.08.011 [PubMed: 17981334]
4. Mwanza JC, Durbin MK, Budenz DL, et al. Profile and predictors of normal ganglion cell-inner plexiform layer thickness measured with frequency-domain optical coherence tomography. Invest Ophthalmol Vis Sci. 2011;52(11):7872–7879. doi:10.1167/iovs.11-7896 [PubMed: 21873658]
5. Verticchio Vercellin AC, Jassim F, Poon LYC, et al. Diagnostic Capability of Three-Dimensional Macular Parameters for Glaucoma Using Optical Coherence Tomography Volume Scans. Invest Ophthalmol Vis Sci. 2018;59(12):4998–5010. doi:10.1167/iovs.18-23813 [PubMed: 30326067]
6. Mohammadzadeh V, Fatehi N, Yarmohammadi A, et al. Macular imaging with optical coherence tomography in glaucoma. Surv Ophthalmol. 2020;65(6):597–638. doi:10.1016/j.survophthal.2020.03.002 [PubMed: 32199939]
7. Liu M, Duggan J, Salt TE, Cordeiro MF. Dendritic changes in visual pathways in glaucoma and other neurodegenerative conditions. Exp Eye Res. 2011;92(4):244–250. doi:10.1016/j.exer.2011.01.014 [PubMed: 21310146]
8. Della Santina L, Inman DM, Lupien CB, Horner PJ, Wong ROL. Differential progression of structural and functional alterations in distinct retinal ganglion cell types in a mouse

model of glaucoma. J Neurosci Off J Soc Neurosci. 2013;33(44):17444–17457. doi:10.1523/JNEUROSCI.5461-12.2013

9. El-Danaf RN, Huberman AD. Characteristic patterns of dendritic remodeling in early-stage glaucoma: evidence from genetically identified retinal ganglion cell types. J Neurosci Off J Soc Neurosci. 2015;35(6):2329–2343. doi:10.1523/JNEUROSCI.1419-14.2015
10. Risner ML, Pasini S, Cooper ML, Lambert WS, Calkins DJ. Axogenic mechanism enhances retinal ganglion cell excitability during early progression in glaucoma. Proc Natl Acad Sci. 2018;115(10):E2393. doi:10.1073/pnas.1714888115 [PubMed: 29463759]
11. Henderson DCM, Vianna JR, Gobran J, et al. Longitudinal In Vivo Changes in Retinal Ganglion Cell Dendritic Morphology After Acute and Chronic Optic Nerve Injury. Invest Ophthalmol Vis Sci. 2021;62(9):5. doi:10.1167/iovs.62.9.5
12. Kim HJ, Lee SY, Park KH, Kim DM, Jeoung JW. Glaucoma Diagnostic Ability of Layer-by-Layer Segmented Ganglion Cell Complex by Spectral-Domain Optical Coherence Tomography. Invest Ophthalmol Vis Sci. 2016;57(11):4799–4805. doi:10.1167/iovs.16-19214 [PubMed: 27654408]
13. Kim EK, Park HYL, Park CK. Segmented inner plexiform layer thickness as a potential biomarker to evaluate open-angle glaucoma: Dendritic degeneration of retinal ganglion cell. PloS One. 2017;12(8):e0182404. doi:10.1371/journal.pone.0182404 [PubMed: 28771565]
14. Moghimi S, Fatehi N, Nguyen AH, Romero P, Caprioli J, Nouri-Mahdavi K. Relationship of the Macular Ganglion Cell and Inner Plexiform Layers in Healthy and Glaucoma Eyes. Transl Vis Sci Technol. 2019;8(5):27. doi:10.1167/tvst.8.5.27
15. Aydın R, Barış M, Durmaz-Engin C, et al. Early localized alterations of the retinal inner plexiform layer in association with visual field worsening in glaucoma patients. PloS One. 2021;16(2):e0247401. doi:10.1371/journal.pone.0247401 [PubMed: 33630899]
16. Ghassabi Z, Kuranov RV, Schuman JS, et al. In Vivo Sublayer Analysis of Human Retinal Inner Plexiform Layer Obtained by Visible-Light Optical Coherence Tomography. Invest Ophthalmol Vis Sci. 2022;63(1):18. doi:10.1167/iovs.63.1.18
17. Beykin G, Norcia AM, Srinivasan VJ, Dubra A, Goldberg JL. Discovery and clinical translation of novel glaucoma biomarkers. Prog Retin Eye Res. 2021;80:100875. doi:10.1016/j.preteyeres.2020.100875 [PubMed: 32659431]
18. Johnson CA, Sample PA, Cioffi GA, Liebmann JR, Weinreb RN. Structure and function evaluation (SAFE): I. criteria for glaucomatous visual field loss using standard automated perimetry (SAP) and short wavelength automated perimetry (SWAP). Am J Ophthalmol. 2002;134(2):177–185. doi:10.1016/s0002-9394(02)01577-5 [PubMed: 12140023]
19. Mohammadzadeh V, Rabiolo A, Fu Q, et al. Longitudinal Macular Structure-Function Relationships in Glaucoma. Ophthalmology. 2020;127(7):888–900. doi:10.1016/j.ophtha.2020.01.023 [PubMed: 32173112]
20. Mohammadzadeh V, Su E, Heydar Zadeh S, et al. Estimating Ganglion Cell Complex Rates of Change With Bayesian Hierarchical Models. Transl Vis Sci Technol. 2021;10(4):15. doi:10.1167/tvst.10.4.15
21. Weiss RE. Modeling Longitudinal Data. Springer New York, NY; 2005.
22. R Core Team. R: A language and environment for statistical computing. R Foundation for Statistical Computing. 2022. Vienna, Austria. https://www.R-project.org/.
23. Plummer M JAGS: A Program for Analysis of Bayesian Graphical Models Using Gibbs Sampling. Proceedings of the 3rd International Workshop on Distributed Statistical Computing. March 20–22, 2003. Vienna, Austria. ISSN 1609–395X.
24. Su YS, Yajima M. R2jags: Using R to run 'JAGS'. Version 0.7–1. August 5, 2021. https://cran.r-project.org/web/packages/R2jags/R2jags.pdf
25. Weinreb RN, Leung CKS, Crowston JG, et al. Primary open-angle glaucoma. Nat Rev Dis Primer. 2016;2:16067. doi:10.1038/nrdp.2016.67
26. Henderson DCM, Vianna JR, Gobran J, et al. Longitudinal In Vivo Changes in Retinal Ganglion Cell Dendritic Morphology After Acute and Chronic Optic Nerve Injury. Invest Ophthalmol Vis Sci. 2021;62(9):5. doi:10.1167/iovs.62.9.5

27. Agostinone J, Alarcon-Martinez L, Gamlin C, Yu WQ, Wong ROL, Di Polo A. Insulin signalling promotes dendrite and synapse regeneration and restores circuit function after axonal injury. Brain J Neurol. 2018;141(7):1963–1980. doi:10.1093/brain/awy142

28. Chien JL, Ghassibi MP, Patthanathamrongkasem T, et al. Glaucoma Diagnostic Capability of Global and Regional Measurements of Isolated Ganglion Cell Layer and Inner Plexiform Layer. J Glaucoma. 2017;26(3):208–215. doi:10.1097/IJG.0000000000000572 [PubMed: 27811573]

29. Hou H, Moghimi S, Kamalipour A, et al. Macular Thickness and Microvasculature Loss in Glaucoma Suspect Eyes. Ophthalmol Glaucoma. Published online July 30, 2021:S2589–4196(21)00180–0. doi:10.1016/j.ogla.2021.07.009

30. Miki A, Medeiros FA, Weinreb RN, et al. Rates of retinal nerve fiber layer thinning in glaucoma suspect eyes. Ophthalmology. 2014;121(7):1350–1358. doi:10.1016/j.ophtha.2014.01.017 [PubMed: 24629619]

31. Chauhan BC, Vianna JR, Sharpe GP, et al. Differential Effects of Aging in the Macular Retinal Layers, Neuroretinal Rim, and Peripapillary Retinal Nerve Fiber Layer. Ophthalmology. 2020;127(2):177–185. doi:10.1016/j.ophtha.2019.09.013 [PubMed: 31668716]

32. Demirkaya N, van Dijk HW, van Schuppen SM, et al. Effect of age on individual retinal layer thickness in normal eyes as measured with spectral-domain optical coherence tomography. Invest Ophthalmol Vis Sci. 2013;54(7):4934–4940. doi:10.1167/iovs.13-11913 [PubMed: 23761080]

33. Nieves-Moreno M, Martínez-de-la-Casa JM, Morales-Fernández L, Sánchez-Jean R, Sáenz-Francés F, García-Feijoó J. Impacts of age and sex on retinal layer thicknesses measured by spectral domain optical coherence tomography with Spectralis. PloS One. 2018;13(3):e0194169. doi:10.1371/journal.pone.0194169 [PubMed: 29522565]

34. Bowd C, Zangwill LM, Weinreb RN, et al. Racial Differences in Rate of Change of Spectral-Domain Optical Coherence Tomography-Measured Minimum Rim Width and Retinal Nerve Fiber Layer Thickness. Am J Ophthalmol. 2018;196:154–164. doi:10.1016/j.ajo.2018.08.050 [PubMed: 30195890]

35. Wessel JM, Horn FK, Tornow RP, et al. Longitudinal analysis of progression in glaucoma using spectral-domain optical coherence tomography. Invest Ophthalmol Vis Sci. 2013;54(5):3613–3620. doi:10.1167/iovs.12-9786 [PubMed: 23633657]

36. Parikh RS, Parikh SR, Sekhar GC, Prabakaran S, Babu JG, Thomas R. Normal age-related decay of retinal nerve fiber layer thickness. Ophthalmology. 2007;114(5):921–926. doi:10.1016/j.ophtha.2007.01.023 [PubMed: 17467529]

37. Burgoyne CF. A biomechanical paradigm for axonal insult within the optic nerve head in aging and glaucoma. Exp Eye Res. 2011;93(2):120–132. doi:10.1016/j.exer.2010.09.005 [PubMed: 20849846]

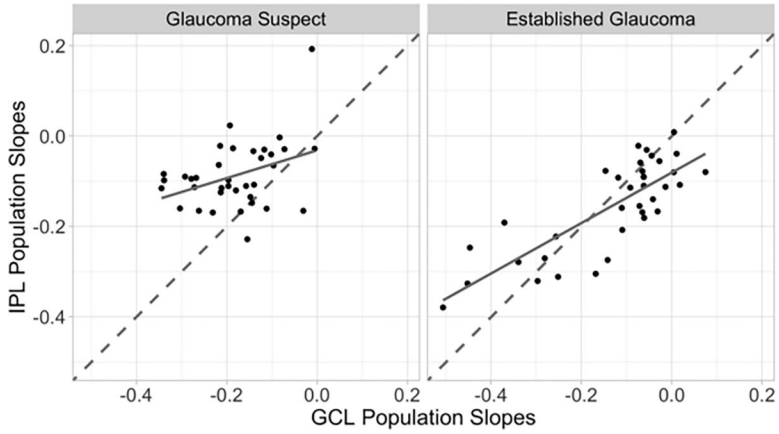

Figure 1.

Posterior mean rates of change for inner plexiform layer (IPL) at each of 36 central macular superpixels plotted against the posterior mean rates of change for ganglion cell layer (GCL) in glaucoma suspect (left) and established glaucoma (right) groups. Dashed line is the line of unity (x=y), the solid line is the least squares regression line for the points in the plot. Points to the left of the dashed line have more negative population GCL slopes than the IPL population slope.

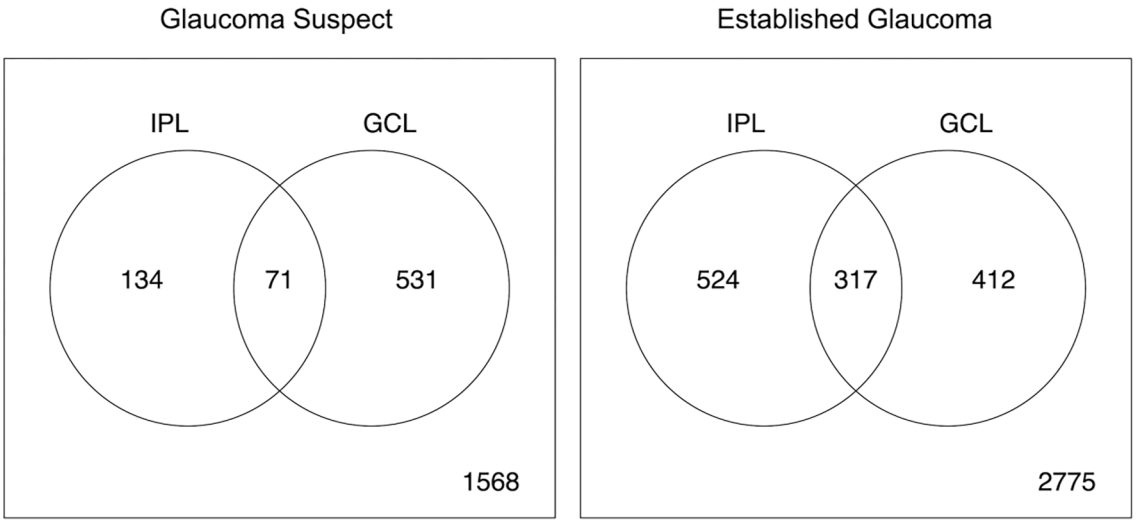

Figure 2.

Venn diagram presents the cross classification of the counts of eye-superpixels with significantly negative (or not) inner plexiform layer (IPL) rates of change and significantly negative (or not) ganglion cell layer (GCL) rates of change within 36 central macular superpixels in the glaucoma suspect (left) and established glaucoma (right) cohorts. Significant negative RoC for an eye-superpixel is defined when the posterior probability that the RoC is negative is greater than 0.9 based on Bayesian hierarchical model.

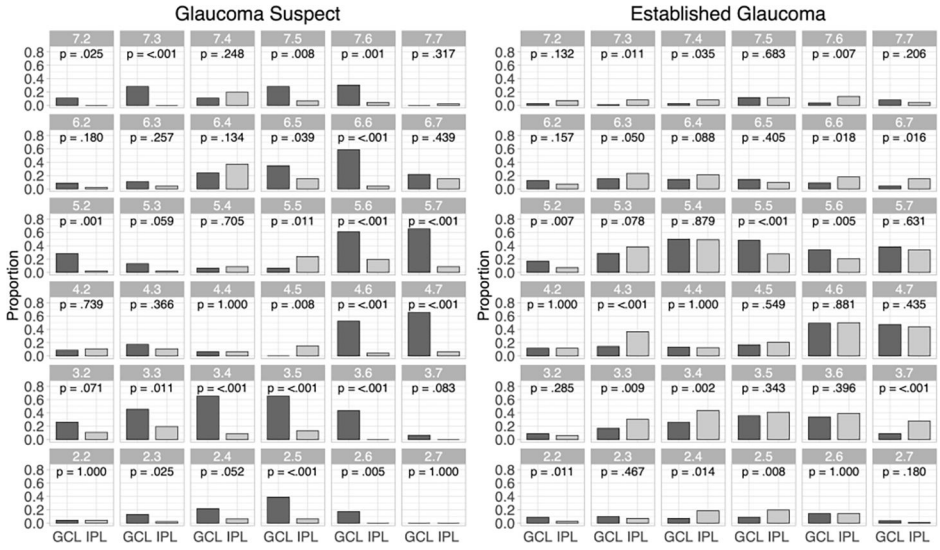

Figure 3.

The proportion of eyes with significantly negative rates of change for ganglion cell layer (GCL) and inner plexiform layer (IPL) for each superpixel for the glaucoma suspect (left) and established glaucoma (right) cohorts (dark gray bars: GCL; light gray bars: IPL). P values for comparison between proportions are based on McNemar's test.

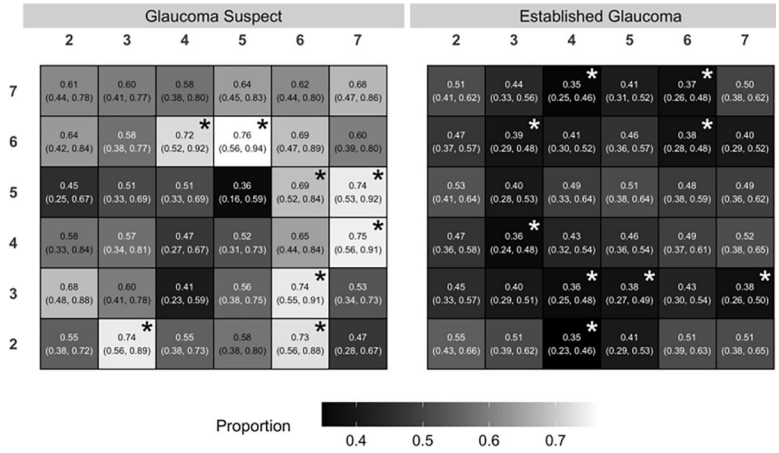

Figure 4.

The proportion of eyes with faster rates of change for ganglion cell layer (GCL) compared to inner plexiform layer (IPL) in each superpixel in the glaucoma suspect (left) and established glaucoma (right) cohorts. A proportion greater than 0.5 denotes a higher likelihood of faster GCL thinning compared to IPL and a proportion less than 0.5 means a higher likelihood of faster IPL thinning compared to GCL. The asterisks flag superpixels where the proportion is significantly above (black) or below (white) 0.5.

Table 1.

Demographic and clinical features of the two patient cohorts.

	GS Cohort	EG Cohort
Number of subjects	46	112
Number of eyes	64	112
No. of OCT scans, mean (SD)	4.2 (1.0)	7.3 (1.1)
Follow-up time (years), mean (SD)	3.5 (0.7)	3.6 (0.4)
Age at baseline, mean (SD)	61.0 (13.7)	66.9 (8.5)
Female gender, n (%)	17 (37.0)	71 (63.4)
Ethnicity, n (%)		
White	29 (63.0)	58 (51.8)
African American	4 (8.7)	16 (14.3)
Hispanic	3 (6.5)	14 (12.5)
Asian	4 (8.7)	24 (21.4)
Other/Unspecified	6 (13.0)	0 (0.0)
24–2 visual field MD (dB), mean (SD)	−0.5 (1.6)	−8.4 (6.9)
24–2 visual field PSD, mean (SD)	1.6 (0.4)	8.3 (3.6)

GS: glaucoma suspect; EG: established glaucoma; MD: mean deviation; PSD: pattern standard deviation